Dynamic subunit stoichiometry confers a progressive continuum of pharmacological sensitivity by KCNQ potassium channels

Haibo Yu[a,b], Zhihong Lin[a,b,1], Margrith E. Mattmann[c,d,e], Beiyan Zou[a,b], Cecile Terrenoire[f], Hongkang Zhang[a,b], Meng Wu[a,b,2], Owen B. McManus[a,b], Robert S. Kass[f], Craig W. Lindsley[c,d,e,g], Corey R. Hopkins[c,d,e,g,3], and Min Li[a,b,3]

[a]The Solomon H. Snyder Department of Neuroscience, High Throughput Biology Center and [b]Johns Hopkins Ion Channel Center, Johns Hopkins University, Baltimore, MD 21205; [c]Department of Pharmacology and [d]Vanderbilt Center for Neuroscience Drug Discovery, Vanderbilt University Medical Center, Nashville, TN 37232; [g]Department of Chemistry and [e]Vanderbilt Specialized Chemistry Center for Probe Development, Vanderbilt University, Nashville, TN 37232; and [f]Department of Pharmacology, Columbia University College of Physicians and Surgeons, New York, NY 10032

Edited by Richard W. Aldrich, University of Texas at Austin, Austin, TX, and approved April 3, 2013 (received for review January 14, 2013)

Voltage-gated KCNQ1 (Kv7.1) potassium channels are expressed abundantly in heart but they are also found in multiple other tissues. Differential coassembly with single transmembrane KCNE beta subunits in different cell types gives rise to a variety of biophysical properties, hence endowing distinct physiological roles for KCNQ1–KCNEx complexes. Mutations in either *KCNQ1* or *KCNE1* genes result in diseases in brain, heart, and the respiratory system. In addition to complexities arising from existence of five KCNE subunits, KCNE1 to KCNE5, recent studies in heterologous systems suggest unorthodox stoichiometric dynamics in subunit assembly is dependent on KCNE expression levels. The resultant KCNQ1–KCNE channel complexes may have a range of zero to two or even up to four KCNE subunits coassembling per KCNQ1 tetramer. These findings underscore the need to assess the selectivity of small-molecule KCNQ1 modulators on these different assemblies. Here we report a unique small-molecule gating modulator, ML277, that potentiates both homomultimeric KCNQ1 channels and unsaturated heteromultimeric $(KCNQ1)_4(KCNE1)_n$ ($n < 4$) channels. Progressive increase of KCNE1 or KCNE3 expression reduces efficacy of ML277 and eventually abolishes ML277-mediated augmentation. In cardiomyocytes, the slowly activating delayed rectifier potassium current, or I_{Ks}, is believed to be a heteromultimeric combination of KCNQ1 and KCNE1, but it is not entirely clear whether I_{Ks} is mediated by KCNE-saturated KCNQ1 channels or by channels with intermediate stoichiometries. We found ML277 effectively augments I_{Ks} current of cultured human cardiomyocytes and shortens action potential duration. These data indicate that unsaturated heteromultimeric $(KCNQ1)_4(KCNE1)_n$ channels are present as components of I_{Ks} and are pharmacologically distinct from KCNE-saturated KCNQ1–KCNE1 channels.

cardiac physiology | drug | long QT | pharmacology

Voltage-gated KCNQ1 (Kv7.1) potassium channels are expressed in cardiac tissue and other nonexcitatory tissues including peripheral epithelial, pancreatic, smooth muscle cells (1, 2), and central nervous system (3). Four identical α-subunits (KCNQ1) form functional channels; however, when coassembled with auxiliary β-subunits (KCNE1), the resultant complex induces a current with biophysical properties similar to cardiac I_{Ks}, a slow component of the delayed rectifier current (4, 5). I_{Ks} is an important component in the repolarizing phase of cardiac action potential. Approximately 50% of long QT patients harbor mutations in either KCNQ1 or KCNE1 genes (6). These patients have a characteristic lengthening of the QT interval in the electrocardiogram that may be caused by delayed cardiac repolarization during action potential (7). More than 300 mutations of KCNQ1 have been annotated in patients and a vast majority of the described mutations are linked to long QT syndrome (8). Loss-of-function mutations of KCNQ1 (LQT1) can result in QT-interval prolongation and enhanced susceptibility to ventricular tachyarrhythmia, notably torsade de pointes. Therefore, pharmacological augmentation of I_{Ks} current represents an effective strategy to understand the physiological roles of this current and may form a basis for development of therapeutics for specific cardiac arrhythmias.

Several pharmacological gating modifiers of KCNQ1 have been reported. These include R-L3 (9, 10), zinc pyrithione (ZnPy) (11) and phenylboronic acid (PBA) (12). However, their specificity for KCNQ1 versus KCNQ1–KCNE complexes remains largely undetermined. R-L3 activates I_{Ks} and shortens action potential duration in guinea pig cardiac myocytes but did not give consistent effects on channels formed by coassembly of KCNQ1 and KCNE1 subunits in a heterologous system (9). ZnPy potentiates KCNQ1 currents but coexpression with KCNE1 ablates this effect (11). PBA augments KCNQ1–KCNE1 complexes at millimolar concentrations with very slow on-rate and off-rate and may act through covalent interactions (12).

Several studies have suggested that KCNQ1 exhibits flexible stoichiometry with KCNE1 varying from one to four subunits per KCNQ1 tetramer, depending on the relative expression levels of the two genes (13–18). More recent experiments with cardiomyocytes differentiated from human stem cells or from induced pluripotent stem cells have shown that the voltage-dependence properties of I_{Ks} fall between KCNQ1 homomultimers and heteromultimeric complexes with saturated KCNE1 levels, further suggesting that I_{Ks} results from coassembled channels with KCNQ1/KCNE1 stoichiometry other than a uniform 4:4 (19, 20).

The flexible stoichiometry of KCNQ1–KCNE channel complexes provides a rationale to examine the roles of KCNE subunits on channel properties and sensitivity to small-molecule modulators. In this study, we used a potent KCNQ1 modulator, ML277 (21), to examine how differential coassembly with KCNE1 modulates the pharmacological properties of KCNQ1–KCNE1 complexes. By testing $(KCNQ1)_4(KCNE1)_n$ channels in a heterologous

Author contributions: H.Y. and M.L. designed research; H.Y., Z.L., B.Z., and M.W. performed research; M.E.M., C.T., R.S.K., C.W.L., and C.R.H. contributed new reagents/analytic tools; H.Y., B.Z., H.Z., M.W., and O.B.M. analyzed data; and H.Y., C.W.L., and M.L. wrote the paper.

The authors declare no conflict of interest.

This article is a PNAS Direct Submission.

Freely available online through the PNAS open access option.

Data deposition: The assays reported in this paper have been deposited in PubChem, http://pubchem.ncbi.nlm.nih.gov (Bioassay Identifier 2699).

[1]Present address: Department of Pharmacology, Carver College of Medicine, University of Iowa, Iowa City, IA 52242.

[2]Present address: High Throughput Screening Facility, Department of Biochemistry, Carver College of Medicine and Department of Pharmaceutical Sciences and Experimental Therapeutics, College of Pharmacy, University of Iowa, Iowa City, IA 52242.

[3]To whom correspondence may be addressed. E-mail: minli@jhmi.edu or corey.r.hopkins@vanderbilt.edu.

This article contains supporting information online at www.pnas.org/lookup/suppl/doi:10.1073/pnas.1300684110/-/DCSupplemental.

expression system and comparing these results with I_{Ks} currents in differentiated human cardiomyocytes, we identified differential pharmacological sensitivity of KCNQ1–KCNE1 complexes at different KCNE1 expression levels. The resultant experimental data provided evidence to interpret pharmacological modulation of I_{Ks} currents by small molecules.

Results

Characterization of ML277 Modulation. ML277 was identified as a KCNQ1 activator in a high-throughput screen for KCNQ1 potassium channel modulators using the NIH Molecular Libraries Small Molecule Repository compound collection (21). ML277 stereo-selectively activates KCNQ1 channels with EC_{50} at submicromolar range. The compound is highly selective against other KCNQ channels by as much as 100-fold over KCNQ2 and KCNQ4 potassium channels (21) and against other heart ion channels including the human *ether-a-go-go* related gene (hERG), Nav1.5, and Cav1.2 (Fig. S1).

To study the mechanism for the potentiating effects of ML277, voltage-dependent channel activation was examined using a CHO cell line expressing human KCNQ1 channels in the absence or presence of ML277 (Fig. 1*A*) by manual patch clamp. At the holding potential of −80 mV, 0.3 μM ML277 induced a rapid increase of KCNQ1 currents elicited by membrane depolarization. The effect attained a maximal level after ML277 was applied for ~7–10 min and was reversible (Fig. 1*B*). The potentiation of ML277 on KCNQ1 is dose-dependent and has an EC_{50} value of 200 ± 20 nM (n = 4–11 for each concentration measurement) for KCNQ1. To determine the voltage-dependent activation, depolarizing voltage steps from −70 mV to +50 mV were applied from holding potential −80 mV for 2 s in 10-mV increments, followed by a hyperpolarizing step to −120 mV to record tail currents. The extrapolated tail current amplitudes were normalized to the maximal tail currents determined after a prepulse to +50 mV and the resulting data were fitted to a Boltzmann function. ML277 induced a hyperpolarizing shift of voltage dependence, in which the half-maximal activation voltage ($V_{1/2}$) was leftward-shifted by 16 mV from control −16.76 ± 0.68 mV (mean ± SEM) to −32.68 ± 1.27 mV. The maximal conductance (G_{max}) was increased sixfold (Fig. 1 *C* and *D*).

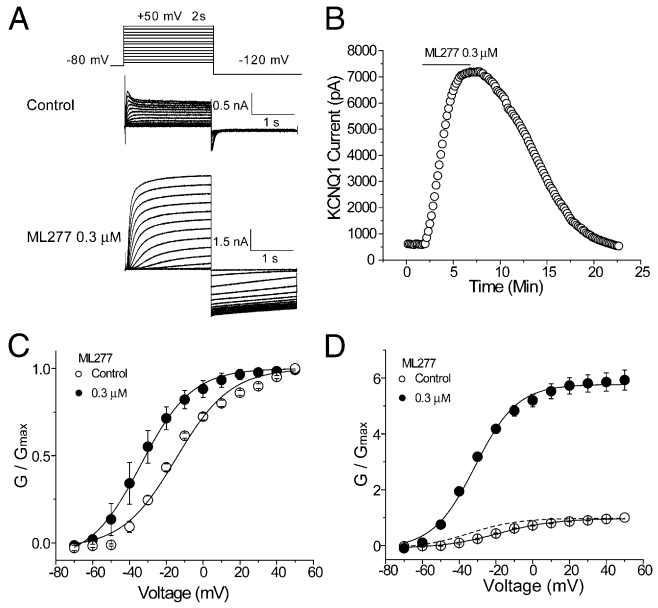

Fig. 1. Characterization of ML277 activation of KCNQ1 currents in KCNQ1–CHO cells using manual patch clamp. (*A*) Representative KCNQ1 current traces in the absence and presence of ML277. (*Inset*) The recording protocol. The cell was held at −80 mV and depolarizing voltage steps from −70 mV to +50 mV were applied for 2 s in 10-mV increments, followed by a hyperpolarizing step to −120 mV. (*B*) Time course of the activation effect of ML277 when steady-state currents were measured. (*C*) Voltage-conductance curves in the absence and presence of ML277, in which the conductance was normalized to the maximal conductance of each treatment (G/G_{max}), presented as mean ± SEM, n = 4–7. (*D*) In the presence of ML277, G_{max} was normalized to the maximal conductance (G_{max}) in the absence of ML277. The dashed line represents the effect of ML277 after rescaling G_{max} to 1 as shown in *C*.

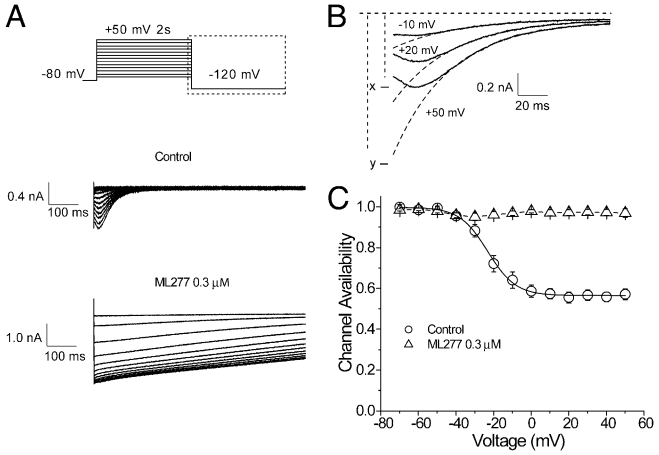

Fig. 2. Effects of ML277 on inactivation kinetics of KCNQ1. (*A*) Representative tail current traces to analyze KCNQ1 inactivation kinetics in the absence and presence of ML277 using the protocol shown (*Inset*). Tail currents were recorded by repolarizing the membrane potential to −120 mV after a series of 2-s depolarizing pulses from −70 mV to +50 mV in 10-mV increments. (*B*) Tail currents measured at −120 mV after a prepulse to −10, +20 and +50 mV. Tail currents were fitted with a single-exponential function (dashed line) to the later phase of the tail current relaxation. Initial current (*x*) and extrapolated (*y*) current are indicated for the currents measured after the prepulse to +50 mV. Horizontal dash line indicates zero current level. (*C*) Voltage-dependent inactivation curves are shown in the absence and presence of ML277, presented as mean ± SEM (n = 4–7).

In addition to voltage-dependent activation, KCNQ1 inactivation kinetics was studied by the same recording protocol outlined in Fig. 1. The voltage dependence of inactivation was determined by the tail current analysis according to an earlier report (22). As shown in Fig. 2*A*, inactivation of KCNQ1 becomes apparent in a hook in the tail currents when repolarizing the membrane potential to −120mV after the depolarizing pulses. The hook is attributed to rapid recovery of channels from inactivation. Two components of tail currents were measured as shown in Fig. 2*B*: an initial tail current (*x*) and an extrapolated current (*y*) determined from a single-exponential fit of tail currents beginning after the initial hook (22). The ratio *x*/*y* was used to estimate channel availability. The half-inactivation voltage was −23.19 ± 0.59 mV under control conditions. In the presence of ML277, the hook in the tail current was no longer visible, indicating a complete removal of voltage-dependent inactivation (Fig. 2*C*).

To quantify the effects of ML277, a Hodgkin–Huxley-type model was used to fit the data (23, 24). It was assumed that KCNQ1 has two independent gates, one controlling activation and the other controlling inactivation. The KCNQ1 steady-state current amplitude can be described by the Hodgkin–Huxley-type equation $I_{KCNQ1} = G_{max}(V - E_K)x_{r1}x_{r2}$. The compound effect on KCNQ1 steady-state current could be interpreted by the alteration in maximal conductance (G_{max}), reversal potential of potassium ion (E_K), activation gate availability (xr1), and inactivation gate availability (xr2) at the given voltages. We did not observe any change of the reversal potential in the presence of ML277. However, the other three parameters (G_{max}, xr1, and xr2) have been altered by

PHARMACOLOGY

ML277. According to the parameters (Table S1) from the voltage-dependent activation and inactivation curves, the gate availability of activation and inactivation were simulated as shown in Fig. S2*A*. The simulated compound effect on KCNQ1 steady-state currents correlates well with the experimental data (Fig. S2*B*). Therefore, the hyperpolarizing shift of half-maximal activation voltage ($V_{1/2}$), significantly increased maximal conductance, and inhibition of inactivation contribute to the overall augmentation of current amplitude.

Incremental Suppression of ML277-Mediated Augmentation by KCNE Subunits. Earlier reports indicated that coassembly of KCNQ1 and KCNE1 form the molecular determinants for cardiac I_{Ks} current (4, 5), a slow component of the delayed rectifier currents that play an important role in repolarizing cardiac cells during action potentials. To study the effects of ML277 on the KCNQ1–KCNE1 complex, we made a stable cell line expressing both KCNQ1 and KCNE1 in a bicistronic vector controlled by the human CMV immediate-early promoter and the human elongation factor 1α-subunit (EF-1α) promoter, respectively (*Materials and Methods*). Differing from KCNQ1 homomultimers, ML277 enhanced the KCNQ1/E1 currents recorded from the cell line by threefold, far less effectively than currents from the KCNQ1 cell line (Fig. S3*A*). In the presence of 0.3 μM ML277, the $V_{1/2}$ was leftward-shifted by 26 mV from control 17.68 ± 1.05 mV to −8.99 ± 1.35 mV (Fig. S3*B*).

Several lines of evidence, especially results from heterologous expression systems, suggest the coassembly of the pore-forming KCNQ1 subunits with auxiliary KCNE1 subunits is incremental depending on the expression and availability of KCNE1 (15, 18). We consider several scenarios for KCNE1 regulation of KCNQ1 sensitivity to ML277 based on the stoichiometry of KCNQ1–E1 complexes. In one scenario, only KCNQ1 homomeric channels are sensitive to ML277, and in this case the lower efficacy of ML277 in the stable cell line is due to the limited number of homomultimeric KCNQ1 channels. In other scenarios, KCNQ1–E1 channels are sensitive to ML277 and sensitivity may depend on the number of KCNE1 channels in the complexes. To examine these possibilities, we chose to transiently express KCNQ1 channels with increasing amounts of KCNE subunits. Cells expressing different ratios of KCNQ1–KCNE1 channels were then examined by electrophysiology. In the absence of KCNE1 expression, a current typical for KCNQ1 homomeric channels was observed (Fig. 3*A*, *Top*). At 1:10 transfection ratio of KCNQ1/KCNE1, we observed a current typical for KCNQ1–KCNE1 as reported earlier (Fig. 3*A*, *Bottom*) (4, 5). At the 1:0.1 ratio of KCNQ1/KCNE1, an apparent mixture of KCNQ1 homomultimers and KCNQ1–KCNE1 heteromultimers was observable (Fig. 3*A*, *Middle*). By examining the voltage-dependence of channel gating, we noted the G–V relationship progressively shifts to more depolarizing voltages at increased levels of KCNE1 (Fig. 3 *B* and *C*). At the 1:1 and 1:10 ratios of KCNQ1/KCNE1, no further shift was observed, indicative that coassembly with KCNE1 reached saturated stoichiometry, presumably $(KCNQ1)_4(KCNE1)_4$ or 4:4 stoichiometry. The progressive stoichiometry from 4:0–4:4 and the heterogeneous intermediate stoichiometry of heteromultimers afforded the opportunity to examine ML277 sensitivity. Indeed, in the absence of KCNE1, ML277 has a maximal effect of more than 10-fold (I/I_0). With increasing levels of KCNE1, the effects were gradually reduced. Eventually, the saturated coassembly of KCNQ1–KCNE1 is no longer sensitive to ML277 (Fig. 3*D*). The midpoint of activation (17.68 ± 1.05 mV, $n = 7$) in the KCNQ1–KCNE1 cell line was between that of KCNQ1 ($V_{1/2} = -17.83 \pm 1.75$mV, $n = 4$) and KCNQ1/KCNE1 channels (plasmid ratio: 1:10) ($V_{1/2} = 29.44 \pm 0.88$mV, $n = 4$) (Fig. S4), which is consistent with the modest potentiation of ML277 on KCNQ1/KCNE1 channels in the cell line.

The diminution of ML277-mediated augmentation is in fact not limited to KCNE1. KCNE3 is another KCNE subunit expressed in human heart (25). Similar experiments using KCNE3 yielded essentially the same results as those using KCNE1 (Fig. 4*A*). There are several small-molecule modulators that augment KCNQ1 channels, although with different potency. Among them, R-L3, or L-364,373 (R)-3-((1H-indol-3-yl)methyl)-5-(2-fluorophenyl)-1-methyl-1H-benzo[e][1,4]diazepin-2(3H)-one, is best characterized (9, 10) and was subject to the same test as outlined in Fig. 3. As shown in Fig. 4*B*, R-L3 was able to increase KCNQ1 homomultimers similar to earlier reported results. Similar to ML277, the saturation of KCNQ1 with KCNE1 gradually abolished the augmentation and eventually eliminated effects.

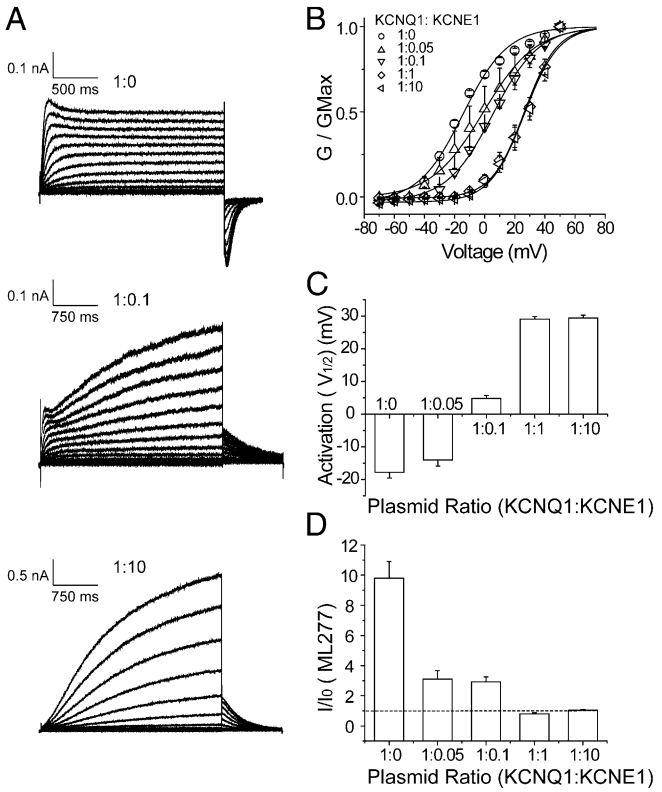

Fig. 3. KCNQ1/KCNE1 complexes lose sensitivity to ML277 when saturated KCNE1 is present. All experiments were completed with transiently transfected cells including WT KCNQ1 alone. (*A*) Representative KCNQ1/KCNE1 traces for KCNQ1/KCNE1 plasmid ratio 1:0, 1:0.1, and 1:10. (*B*) Voltage-conductance curves for different ratio of KCNQ1/KCNE1. (*C*) Bar graph of half-activation voltages for different ratios of KCNQ1/KCNE1. (*D*) Effect of 0.3 μM ML277 on the different ratios of KCNQ1:KCNE1 ($n = 3$–7). The KCNQ1 currents were measured at the test voltage +50mV. Data are presented as mean ± SEM.

Given the sensitivity of 4:0 channels but lack of sensitivity for the putative 4:4 KCNE-saturated channels, we then asked whether the heteromultimeric channels are sensitive to ML277. Under limited KCNE1 expression, one can estimate the ratio of $(KCNQ1)_4$ homomultimers relative to a cohort of mixed $(KCNQ1)_4(KCNE1)_n$ ($n < 4$) heteromultimers because fast activation is seen only in KCNQ1 homomultimers (26). However, in transfected cells with different plasmid ratios, it was not consistently reliable to resolve the fraction of homomultimers from those heteromultimers based on the kinetic signature of fast activation. Earlier studies have provided evidence that a tandem fusion of KCNE1–KCNQ1–KCNQ1(EQQ) and KCNE1–KCNQ1(EQ) could confine specific stoichiometries of $(KCNQ1)_4(KCNE1)_2$ and $(KCNQ1)_4(KCNE1)_4$ (15, 27). Therefore, we tested the effects of ML277 on these constructs. As shown in Fig. 5*A*, *Top* and *Middle*, EQ was activated at the more depolarized voltages relataive to EQQ and the time

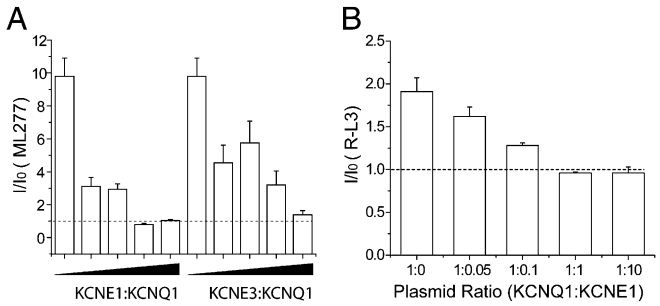

Fig. 4. KCNEx subunits reduce the sensitivity of KCNQ1 to activators. (*A*) A bar graph shows effects of 0.3 μM ML277 on different ratios of KCNQ1 and KCNE subunits (KCNE1 or KCNE3). The ratios of KCNQ1:KCNE1 are 1:0, 1:0.05, 1:0.1, 1:1, and 1:10 from left to right. The ratios of KCNQ1:KCNE3 are 1:0, 1:1, 1:10, 1:50, and 1:100 from left to right. (n = 3–9). (*B*) KCNQ1/KCNE1 loses sensitivity to R-L3 when saturated KCNE1 dose was present. All experiments were performed with transiently transfected cells including wt KCNQ1 alone. The bar graph shows the effects of R-L3 on the different combinations of KCNQ1:KCNE1 ratios. (n = 3–7). The KCNQ1 currents were measured at the test voltage +50mV. Data are presented as mean ± SEM.

course of activation was slower than EQQ (Fig. 5*A*, *Bottom*). The $V_{1/2}$ of EQQ (14.10 ± 0.81mV) falls between KCNQ1 alone (−17.83 ± 1.75 mV) and KCNQ1/KCNE1 (1:1) (29.10 ± 0.77 mV). The $V_{1/2}$ of EQ (26.44 ± 0.73 mV) was similar to that of KCNQ1:KCNE1 1:1 (Fig. 5 *B* and *C*). Similar to the data from KCNQ1:KCNE1 ratios of 1:0.05 and 1:0.1, EQQ currents were increased by 1.61-fold but the extent of increase is smaller than the others (Fig. 5*D*). EQ currents were not sensitive to ML277 even when the concentration was increased to 10 μM. With the increase of KCNE1 amount in the KCNQ1–KCNE1 complex, ML277 gradually decreased its effect. Measurement of EC_{50} shows 200 ± 20 nM (KCNQ1) and 152 ± 22 nM (EQQ) channels (Fig. 5*E*). Therefore, ML277 is most effective on $(KCNQ1)_4$ but less effective on $(KCNQ1)_4(KCNE1)_n$ ($n < 4$) complexes. The difference is not due to any major change in apparent affinity, but rather to the reduced efficacy.

Augmentation of I_{Ks} in Human Cardiomyocytes. I_{Ks} is formed by heteromultimeric KCNQ1–KCNE1 channels. We first studied the effects of ML277 on action potential duration (APD) using induced pluripotent stem cell (iPSC)-derived cardiomyocytes. The experiments were carried out using spontaneously beating cardiomyocytes with ventricular-like action potentials (24). Because ML277 is not effective for the KCNE-saturated putative $(KCNQ1)_4(KCNE1)_4$ channels, we would anticipate no effects. In contrast, we noted significant shortening of the APDs (Fig. 6 *A* and *B*). The shortening effects were dose-dependent with an estimated EC_{50} at 106 nM, comparable to the EC_{50} obtained from a heterologous expression system, supporting ML277 acts on I_{Ks} (Fig. 6*C*). To examine whether APD shortening is due to the augmentation of native potassium currents, especially I_{Ks}, single-cell voltage clamp experiments were performed using isolated individual cardiomyocytes. In these experiments, other currents, including I_{Na}, I_{to}, I_{K1}, I_{Ca}, and I_{Kr}, were pharmacologically suppressed (*Materials and Methods*). The representative current traces for transfected KCNQ1:KCNE1 (1:0.1) and cardiomyocyte I_{Ks} were recorded at the same testing voltage as shown in Fig. 6*D*. ML277 enhanced chromanol-sensitive and voltage-dependent potassium currents in the presence of E-4031, a specific inhibitor for I_{Kr} (Fig. 6*E*). Chromanol 293B was applied at 10 μM in the cardiomyocyte recording, which is close to ~70% inhibition on I_{Ks} currents (28). These results combined with counter screen tests (Fig. S1) against other cardiac ion channels argue for selective augmentation of I_{Ks} by ML277, hence shortening APD.

Discussion

Several classes of small-molecule activators for KCNQ channels have been identified and they differ in chemical structure, mode of action, and target selectivity (29–34). For example, among five KCNQ channels, KCNQ1 to KCNQ5 (or Kv7.1–Kv7.5), Retigabine has a rank order of potency as KCNQ3 > KCNQ2 > KCNQ4 = KCNQ5 >> KCNQ1 according to the available data (34), whereas ZnPy has a rank order of efficacy as KCNQ4 >> KCNQ2 > KCNQ1 >> KCNQ3 (32). Retigabine and ZnPy recognize two distinct molecular sites (32, 33, 35, 36). Indeed, different homomultimers and heteromultimers have been found among KCNQ2 and KCNQ5 subunits, especially in the nervous system. So far, there is no evidence that one nonsensitive subunit dominantly diminishes sensitivity to chemical modulators in heteromultimers. In addition to little expression overlap between KCNQ1 and the other KCNQ family members, coassembly with KCNE has only been observed with KCNQ1 subunits. KCNE seems to act dominantly in that, at saturated expression levels, the ML277 and R-L3 effects were no longer observable.

Although our experiments could not specify that the saturated form is $(KCNQ1)_4(KCNE1)_4$ stoichiometry, the progressive

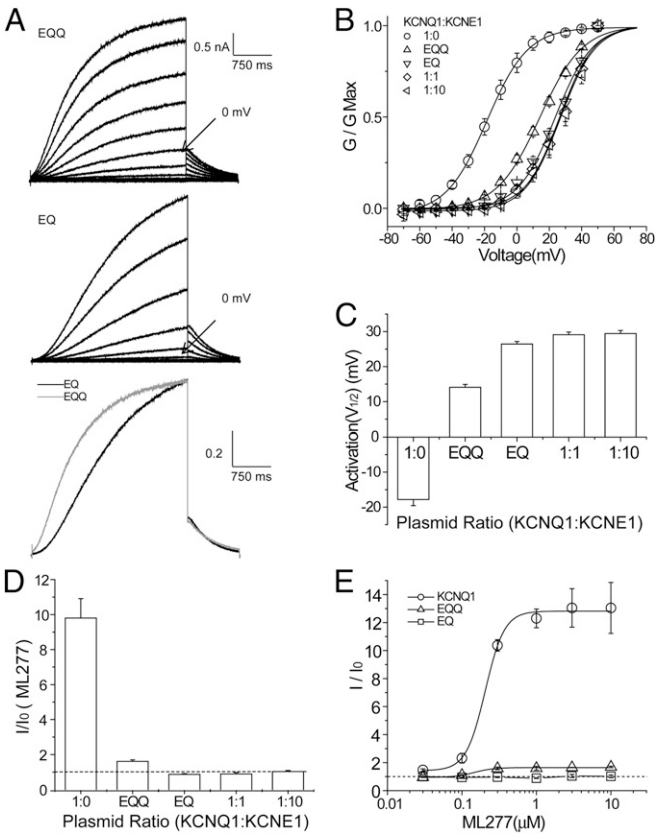

Fig. 5. ML277 activated unsaturated but not saturated KCNQ1–KCNE1 complexes. All experiments were completed with transiently transfected cells. (*A*) Representative current traces of EQQ and EQ. The arrows indicate the current level at the depolarization voltage 0 mV (*Top* and *Middle*). The superimposed EQ and EQQ current traces at +50 mV to compare the activation time course, in which the current has been normalized to the maximal currents in each cell (*Lower*). (*B*) Voltage-conductance curves for different ratios of KCNQ1:KCNE1. EQQ represented KCNQ1:KCNE1 plasmid ratio 1:0.5 and EQ for 1:1 ratio. (*C*) Bar graph of half-activation voltages for different ratios of KCNQ1:KCNE1. (*D*) Effect of 0.3 μM ML277 on the different ratios of KCNQ1:KCNE1 (n = 3–7). The KCNQ1 currents were measured at the test voltage +50mV. Data are presented as mean ± SEM. (*E*) Dose-dependent curves of ML277 on KCNQ1, EQQ, and EQ (n = 4–10).

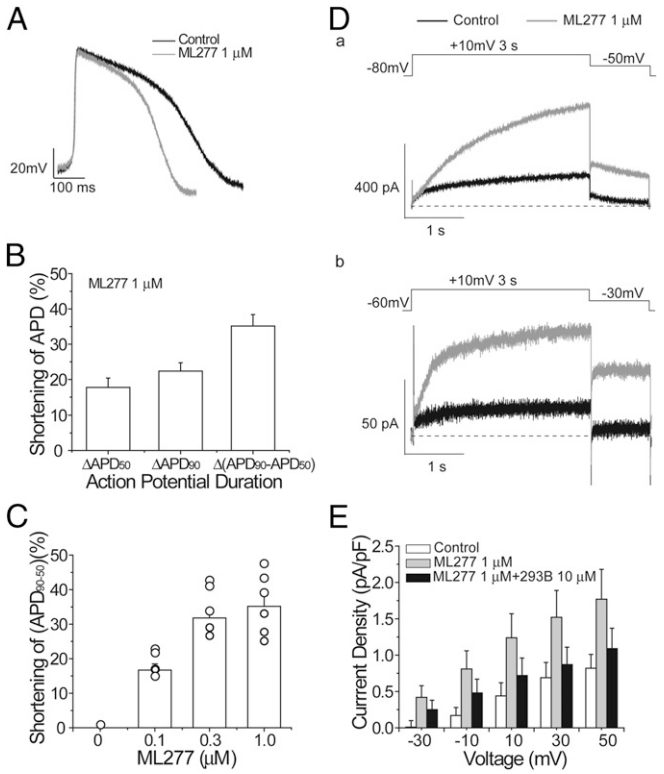

Fig. 6. ML277 shortened the action potential duration by increasing potassium currents in iPSC-derived cardiomyocytes. (*A*) Superimposed representative single action potential traces in the absence and presence of 1 μM ML277. (*B*) Effect of ML277 on the action potential durations (n = 6). (*C*) Dose-dependent effect of ML277 on the shortening of action potential duration ($APD_{90–50}$) (n = 5–9). (*D*) Representative current traces for KCNQ1/KCNE1 currents. Current traces (*D*, *a*) from transfection molecular ratio 1:0.1 in the CHO-K1 cells and I_{Ks} currents (*D*, *b*) from iPSC-derived cardiomyocytes in the absence and presence of ML277. The recording voltage was same for the two sets of cells. (*E*) Compound effects on steady-state currents. The holding potential was −60 mV. The steady-state current was examined from −30mV to +50mV in 20-mV increments. Except for I_{Ks}, other major ionic components including I_{Na}, I_{Kr}, I_{K1}, I_{to}, and I_{CaL} were pharmacologically suppressed. ML277-activated currents were chromanol-sensitive. Data are presented as mean ± SEM.

reduction in sensitivity as a function of increasing expression of KCNE1 or KCNE3 may explain the discrepancy concerning R-L3 effects: R-L3 activates I_{Ks} and shortens action potential duration in guinea pig cardiac myocytes but does not affect channels formed by coassembly of KCNQ1 and KCNE1 subunits in *Xenopus* oocytes (9). The data reported here indicate R-L3 is effective on unsaturated $(KCNQ1)_4(KCNE1)_n$ channels but not the saturated putative $(KCNQ1)_4(KCNE1)_4$ channels. One possible explanation is that coexpression in oocytes resulted in a majority of saturated KCNQ1/KCNE1 channels. Indeed, an earlier study in *Xenopus* oocytes reports progressive gating change depending on expression levels of KCNE1, presumably through coassembly with endogenous KCNQ1 (37). Admittedly, based on the experimental design one cannot precisely determine whether all unsaturated forms $(KCNQ1)_4(KCNE1)_n$ ($n < 4$) are sensitive to ML277. This information will require expression and assembly of KCNQ1–KCNE1 in a defined stoichiometry.

It is important to note that the precise stoichiometry of native KCNQ1:KCNEx is still a subject of some debate. The experimental evidence for both flexible $(KCNQ1)_4(KCNEx)_n$ (where n = 0, 1, 2, 3, or 4) stoichiometry and more fixed $(KCNQ1)_4(KCNEx)_2$ stoichiometry have been obtained using different experimental systems or fusion protein constructs (13–15, 18). As referenced above, the evidence in this report does not identify the stoichiometry of the subunits. However, our data suggest that KCNE1, depending expression level, assembles with KCNQ1 in different stoichiometries that progressively alter the pharmacological sensitivity. Therefore, our data are consistent with, but do not prove, an unsaturated assembly such as $(KCNQ1)_4(KCNE1)_2$.

The molecular determinants for I_{Ks} include both KCNQ1 and KCNE1 subunits (4, 5). Indeed, spatial and temporal expression changes of the corresponding genes have been noted in human heart (38, 39). There are reports on differential I_{Ks} pharmacology in epicardium, midmyocardium, and endocardium (40). The demonstration of incremental heteromultimers in transfected cells (15) and in cultured human cardiomyocytes (19, 20) has provided direct support for their roles in endowing diverse I_{Ks} currents. The specificity for certain stoichiometries by ML277 and R-L3 adds independent evidence for the existence of unsaturated heteromultimeric channels in human cardiomyocytes. Given the widespread tissue expression of KCNQ1 and its ability to coassemble with at least one of the five KCNE subunits, it would be interesting to examine whether the observation reported for KCNE1 and KCNE3 is generalizable to other KCNE subunits and in different tissues. Indeed, KCNE subunits primarily affect KCNQ1. However, there are reports, for example, suggesting that KCNEs affect other Kv channels, including Kv4.2 (41). It would also be interesting to determine whether the specificity for unsaturated KCNQ1/KCNE stoichiometry is in fact applicable to or different from that by other allosteric modulators (42, 43), including ones discovered recently (12, 44). The continuum of incremental subunit coassembly and that of differential pharmacological sensitivity to small-molecule modulators highlight both complexity of the regulation and opportunities to develop therapeutic interventions.

Materials and Methods

Cell Culture. The stable cell lines expressing KCNQ1 and hERG were previously generated using CHO cells. The KCNQ1/KCNE1 stable cell line was made expressing both KCNQ1 and KCNE1 in a bicistronic vector controlled by the human CMV immediate-early promoter and the human EF-1α promoter, respectively. The cell lines for cardiac ion channels Nav1.5 and Cav1.2 were made in HEK-293 cells. These cells were routinely cultured in 50/50 DMEM/F12 (Mediatech) with 10% (vol/vol) FBS (Gemini Bio Products) and 2 mM L-glutamine (Invitrogen). Cells were maintained and passaged when reaching 80% confluency. CHO cells stably expressing hERG were grown in F12 and GlutaMAX (Invitrogen) with 10% FBS (Gemini Bio Products).

The iPSC-derived cardiomyocytes (healthy control) were obtained from Cellular Dynamics Inc. They were cultured at 37 °C with 5% CO_2 according to the manufacturer's recommended protocol. Briefly, the cells at differentiation day 32 were thawed and seeded in the manufacturer-provided medium on 0.1% gelatin-coated plates. At 48 h after seeding, cell debris was removed and cells were cultured in maintenance medium (Cellular Dynamics Inc.). Cells were dislodged and plated on 0.1% gelatin-coated coverslips at 96 h after seeding. Electrophysiological recordings were performed at 48 h after cell replating.

Manual Patch-Clamp Recording in Cell Lines, Transient-Transfected Cells, and iPSC-Derived Cardiomyocytes. To express KCNQ1 and KCNQ1–KCNEx complex, cells were transfected in different plasmid ratios between KCNQ1 and KCNE1 or KCNE3 using Lipofectamine LTX with Plus Reagent according to the manufacture's instruction (Invitrogen). A plasmid expressing EGFP was cotransfected to identify transfection-positive cells. After transfection for 24 h, cells were split and replated onto coverslips coated with poly-L-lysine (Sigma). At 48–72 h after transfection, the cells were used for electrophysiological recording.

Traditional whole-cell voltage clamp recording was performed at room temperature to record the KCNQ1, KCNQ1/KCNE1, hERG, Nav1.5, and Cav1.2 currents. Cells were seeded in 35-mm culture dishes at a low density 1 d before recording. Recording pipettes were pulled with borosilicate glass (World Precision Instruments Inc.) to 2–5 MΩ when filled with a pipette solution containing 145 mM KCl, 1 mM $MgCl_2$, 5 mM EGTA, 10 mM Hepes, and 5 mM MgATP at pH 7.2 and placed in a bath solution containing 140 mM NaCl, 5 mM KCl, 2 mM $CaCl_2$, 1.5 mM $MgCl_2$, 10 mM glucose, and 10 mM Hepes at pH 7.4 adjusted with NaOH. Isolated cells were voltage-clamped in whole-cell mode with an AxoPatch 200B amplifier (Molecular Devices Corp.) and

currents were recorded at 10 kHz. Cells were continuously perfused with bath solution through a gravity-driven perfusion system (ALA Scientific). Stock solutions of all chemicals were made with DMSO. Immediately before each experiment, drugs were diluted in appropriate external solutions to desired concentrations and applied by perfusion. Recordings were performed at room temperature (22–25 °C).

To record the spontaneous action potentials (sAPs) from differentiated cardiac myocytes, the Giga-Ohm seal was achieved under the voltage clamp mode and the sAPs were collected under the current clamp configuration using an Axopatch-200A amplifier (Molecular Devices). Cardiomyocyte clusters of 5–20 cells with spontaneous contractions were selected for recordings. Perforated patch was used to prolong recording stability. Pipette solution contained 120 mM KCl, 1 mM $MgCl_2$, 10 mM EGTA, 10 mM Hepes, and 3 mM MgATP at pH 7.2 adjusted with KOH. Amphotericin B (Sigma) at 500 μg/mL was included in the pipette solution. The extracellular buffer is the modified Tyrode's solution containing 140 mM NaCl, 5.4 mM KCl, 1.3 mM $CaCl_2$, 0.5 mM $MgCl_2$, 5 mM Hepes, and 5.5 mM glucose at pH 7.4 adjusted with NaOH. Recordings were performed at 30 °C. Junction potentials were subtracted after recording. To examine compound effects on native I_{Ks} currents, traditional whole-cell voltage-clamp recording was used. For voltage-clamp studies of I_{Ks}, external Na^+ was replaced by equimolar choline (126 mM) and the solution was supplemented by 4-AP (5 mM), $BaCl_2$ (0.5 mM), $CdCl_2$ (0.2 mM), and E-4031 (5 μM) to suppress potential interference of I_{Na}, I_{to}, I_{K1}, I_{Ca}, and I_{Kr}, respectively. I_{Ks} was defined as the chromanol-293B–sensitive (10 μM) current and was elicited by 3-s depolarizing steps from a holding potential of −60mV to potentials ranging from −30 mV to + 50 mV in 20-mV increments. Electrical signals were filtered at 2 kHz and acquired with pClamp 9.2 software via a DigiData-1322A interface (Molecular Devices Corp.).

Data Analysis. Patch-clamp data were processed in Clampfit 9.2 and then analyzed in Excel and Origin 6.0. To determine the voltage dependence of KCNQ1 channel activation, a single-exponential function was fitted to the later phase of tail currents, extrapolated to the beginning of the repolarizing step, and this value (I) normalized to the maximum extrapolated tail current (I_{max}), chord conductance (G) was calculated by using the following equation: $G = I/(V - V_{rev})$.The activation curve was fitted by the Boltzmann equation: $G = (G_{max} - G_{min})/(1 + \exp(V - V_{1/2})/S) + G_{min}$, where G_{max} is the maximum conductance, G_{min} is the minimum conductance, $V_{1/2}$ is the voltage for half of the total number of channels to open, and S is the slope factor. The current amplitude at the test voltage with G_{max} was also used for comparison. The dose–response curve was fitted by the Hill equation in Origin software: $E = E_{max}/(1 + (IC_{50}/C)^{P})$, where E_{max} is the maximum response, C is the drug concentration, IC_{50} is the drug concentration producing half of the maximum response, and P is the Hill coefficient.

Chemicals. Individual compounds used were either synthesized at the Vanderbilt Specialized Chemistry Center or acquired from commercial sources including Sigma and Tocris. Compound stock was prepared in DMSO at 10 mM.

ACKNOWLEDGMENTS. We thank members of the M.L. laboratory for valuable discussions and comments on the manuscript and Alison Neal for editorial assistance. This work was supported by National Institutes of Health and Molecular Libraries Probe Production Centers Network (MLPCN) Grants U54MH084691 (to M.L.), U54MH084659 (to C.W.L.), 5R01HL044365-20 (to R.S.K.), and 1R03MH090837-01 (to M.W.). Johns Hopkins University is a member of the MLPCN and houses the Johns Hopkins Ion Channel Center. Vanderbilt University is a member of the MLPCN and houses the Vanderbilt Specialized Chemistry Center for Accelerated Probe Development.

1. Demolombe S, et al. (2001) Differential expression of KvLQT1 and its regulator IsK in mouse epithelia. *Am J Physiol Cell Physiol* 280(2):C359–C372.
2. Soldovieri MV, Miceli F, Taglialatela M (2011) Driving with no brakes: Molecular pathophysiology of Kv7 potassium channels. *Physiology (Bethesda)* 26(5):365–376.
3. Goldman AM, *et al.* (2009) Arrhythmia in heart and brain: KCNQ1 mutations link epilepsy and sudden unexplained death. *Sci Transl Med* 1(2):2ra6.
4. Barhanin J, et al. (1996) K(V)LQT1 and IsK (minK) proteins associate to form the I(Ks) cardiac potassium current. *Nature* 384(6604):78–80.
5. Sanguinetti MC, et al. (1996) Coassembly of K(V)LQT1 and minK (IsK) proteins to form cardiac I(Ks) potassium channel. *Nature* 384(6604):80–83.
6. Hedley PL, et al. (2009) The genetic basis of long QT and short QT syndromes: a mutation update. *Hum Mutat* 30(11):1486–1511.
7. Wang Q, et al. (1996) Positional cloning of a novel potassium channel gene: KVLQT1 mutations cause cardiac arrhythmias. *Nat Genet* 12(1):17–23.
8. Peroz D, et al. (2008) Kv7.1 (KCNQ1) properties and channelopathies. *J Physiol* 586(7): 1785–1789.
9. Salata JJ, et al. (1998) A novel benzodiazepine that activates cardiac slow delayed rectifier K+ currents. *Mol Pharmacol* 54(1):220–230.
10. Seebohm G, Pusch M, Chen J, Sanguinetti MC (2003) Pharmacological activation of normal and arrhythmia-associated mutant KCNQ1 potassium channels. *Circ Res* 93(10):941–947.
11. Gao Z, Xiong Q, Sun H, Li M (2008) Desensitization of chemical activation by auxiliary subunits: Convergence of molecular determinants critical for augmenting KCNQ1 potassium channels. *J Biol Chem* 283(33):22649–22658.
12. Mruk K, Kobertz WR (2009) Discovery of a novel activator of KCNQ1-KCNE1 K channel complexes. *PLoS ONE* 4(1):e4236.
13. Chen H, Kim LA, Rajan S, Xu S, Goldstein SA (2003) Charybdotoxin binding in the I(Ks) pore demonstrates two MinK subunits in each channel complex. *Neuron* 40(1):15–23.
14. Morin TJ, Kobertz WR (2008) Counting membrane-embedded KCNE beta-subunits in functioning K+ channel complexes. *Proc Natl Acad Sci USA* 105(5):1478–1482.
15. Nakajo K, Ulbrich MH, Kubo Y, Isacoff EY (2010) Stoichiometry of the KCNQ1 - KCNE1 ion channel complex. *Proc Natl Acad Sci USA* 107(44):18862–18867.
16. Osteen JD, Sampson KJ, Kass RS (2010) The cardiac IKs channel, complex indeed. *Proc Natl Acad Sci USA* 107(44):18751–18752.
17. Wang KW, Goldstein SA (1995) Subunit composition of minK potassium channels. *Neuron* 14(6):1303–1309.
18. Wang W, Xia J, Kass RS (1998) MinK-KvLQT1 fusion proteins, evidence for multiple stoichiometries of the assembled IsK channel. *J Biol Chem* 273(51):34069–34074.
19. Wang K, et al. (2011) Biophysical properties of slow potassium channels in human embryonic stem cell derived cardiomyocytes implicate subunit stoichiometry. *J Physiol* 589(Pt 24):6093–6104.
20. Wang M, Kass RS (2012) Stoichiometry of the slow I(ks) potassium channel in human embryonic stem cell-derived myocytes. *Pediatr Cardiol* 33(6):938–942.
21. Mattmann ME, et al. (2012) Identification of (R)-N-(4-(4-methoxyphenyl)thiazol-2-yl)-1-tosylpiperidine-2-carboxamide, ML277, as a novel, potent and selective K(v)7.1 (KCNQ1) potassium channel activator. *Bioorg Med Chem Lett* 22(18):5936–5941.
22. Tristani-Firouzi M, Sanguinetti MC (1998) Voltage-dependent inactivation of the human K+ channel KvLQT1 is eliminated by association with minimal K+ channel (minK) subunits. *J Physiol* 510(Pt 1):37–45.
23. Hodgkin AL, Huxley AF (1952) A quantitative description of membrane current and its application to conduction and excitation in nerve. *J Physiol* 117(4):500–544.
24. Zhang H, et al. (2012) Modulation of hERG potassium channel gating normalizes action potential duration prolonged by dysfunctional KCNQ1 potassium channel. *Proc Natl Acad Sci USA* 109(29):11866–11871.
25. Bendahhou S, et al. (2005) In vitro molecular interactions and distribution of KCNE family with KCNQ1 in the human heart. *Cardiovasc Res* 67(3):529–538.
26. Melman YF, Um SY, Krumerman A, Kagan A, McDonald TV (2004) KCNE1 binds to the KCNQ1 pore to regulate potassium channel activity. *Neuron* 42(6):927–937.
27. Chan PJ, et al. (2012) Characterization of KCNQ1 atrial fibrillation mutations reveals distinct dependence on KCNE1. *J Gen Physiol* 139(2):135–144.
28. Bosch RF, et al. (1998) Effects of the chromanol 293B, a selective blocker of the slow, component of the delayed rectifier K+ current, on repolarization in human and guinea pig ventricular myocytes. *Cardiovasc Res* 38(2):441–450.
29. Schrøder RL, et al. (2001) KCNQ4 channel activation by BMS-204352 and retigabine. *Neuropharmacology* 40(7):888–898.
30. Wickenden AD, Yu W, Zou A, Jegla T, Wagoner PK (2000) Retigabine, a novel anticonvulsant, enhances activation of KCNQ2/Q3 potassium channels. *Mol Pharmacol* 58(3):591–600.
31. Wickenden AD, Zou A, Wagoner PK, Jegla T (2001) Characterization of KCNQ5/Q3 potassium channels expressed in mammalian cells. *Br J Pharmacol* 132(2):381–384.
32. Xiong Q, Sun H, Li M (2007) Zinc pyrithione-mediated activation of voltage-gated KCNQ potassium channels rescues epileptogenic mutants. *Nat Chem Biol* 3(5):287–296.
33. Xiong Q, Sun H, Zhang Y, Nan F, Li M (2008) Combinatorial augmentation of voltage-gated KCNQ potassium channels by chemical openers. *Proc Natl Acad Sci USA* 105(8): 3128–3133.
34. Gunthorpe MJ, Large CH, Sankar R (2012) The mechanism of action of retigabine (ezogabine), a first-in-class K+ channel opener for the treatment of epilepsy. *Epilepsia* 53(3):412–424.
35. Schenzer A, et al. (2005) Molecular determinants of KCNQ (Kv7) K+ channel sensitivity to the anticonvulsant retigabine. *J Neurosci* 25(20):5051–5060.
36. Wuttke TV, Seebohm G, Bail S, Maljevic S, Lerche H (2005) The new anticonvulsant retigabine favors voltage-dependent opening of the Kv7.2 (KCNQ2) channel by binding to its activation gate. *Mol Pharmacol* 67(4):1009–1017.
37. Cui J, Kline RP, Pennefather P, Cohen IS (1994) Gating of IsK expressed in *Xenopus* oocytes depends on the amount of mRNA injected. *J G Physiol* 104:87–105.
38. Gaborit N, et al. (2007) Regional and tissue specific transcript signatures of ion channel genes in the non-diseased human heart. *J Physiol* 582(Pt 2):675–693.
39. Lundquist AL, et al. (2005) Expression of multiple KCNE genes in human heart may enable variable modulation of I(Ks). *J Mol Cell Cardiol* 38(2):277–287.
40. Li Y, et al. (2003) Effect of imidapril on heterogeneity of slow component of delayed rectifying K+ current in rabbit left ventricular hypertrophic myocytes. *Acta Pharmacol Sin* 24(7):681–686.
41. Liu WJ, et al. (2008) Co-expression of KCNE2 and KChIP2c modulates the electrophysiological properties of Kv4.2 current in COS-7 cells. *Acta Pharmacol Sin* 29(6):653–660.
42. Wulff H, Castle NA, Pardo LA (2009) Voltage-gated potassium channels as therapeutic targets. *Nat Rev Drug Discov* 8(12):982–1001.
43. Xiong Q, Gao Z, Wang W, Li M (2008) Activation of Kv7 (KCNQ) voltage-gated potassium channels by synthetic compounds. *Trends Pharmacol Sci* 29(2):99–107.
44. Zheng Y, et al. (2012) Hexachlorophene is a potent KCNQ1/KCNE1 potassium channel activator which rescues LQTs mutants. *PLoS ONE* 7(12):e51820.